AJNR

Subdural grid implantation for intracranial EEG recording: CT and MR appearance.

M A Silberbusch, M I Rothman, G K Bergey, G H Zoarski and M T Zagardo

AJNR Am J Neuroradiol 1998, 19 (6) 1089-1093
http://www.ajnr.org/content/19/6/1089

AJNR Am J Neuroradiol 19:1089–1093, June 1998

Subdural Grid Implantation for Intracranial EEG Recording: CT and MR Appearance

M. A. Silberbusch, M. I. Rothman, G. K. Bergey, G. H. Zoarski, and M. T. Zagardo

PURPOSE: **Subdural grid arrays are used when seizure activity cannot be located by ictal scalp recordings and when functional cortical mapping is required before surgery. This study was performed to determine and compare the CT and MR imaging appearance of subdural EEG grids and to identify the types and frequency of associated complications.**

METHODS: **We retrospectively reviewed the medical records and imaging studies of 51 consecutive patients who underwent 54 craniotomies for subdural EEG grid implantation with either stainless steel or platinum alloy contacts between June 1988 and September 1993. Twenty-two patients had both CT and MR examinations, 27 patients had CT only, and five patients had MR imaging only. All studies were assessed for image quality and degradation by the implanted EEG grids, for intra- and extraaxial collections, and for mass effect, with differences of opinion resolved by consensus.**

RESULTS: **Subdural EEG grids caused extensive streak artifacts on all CT scans (corresponding directly to grid composition) and mild to moderate magnetic susceptibility artifacts on MR images. Sixteen associated complications were detected among the 54 patients imaged, including four significant extraaxial hematomas, four subfalcine or transtentorial herniations, two tension pneumocephali, two extraaxial CSF collections, two intraparenchymal hemorrhages, and one case each of cerebritis and brain abscess.In all but four cases, the detected complications were not clinically apparent and did not require specific treatment. There were no residual sequelae.**

CONCLUSION: **Because of extensive streak artifacts, CT showed only gross complications, such as herniation and grid displacement by extraaxial collections. MR imaging artifacts were more localized, allowing superior evaluation of subdural EEG grid placement and associated complications.**

The presurgical evaluation of patients with intractable epilepsy typically involves the recording and analyzing of seizure activity in order to locate the seizure focus or epileptogenic zone. When scalp recordings are not sufficient, recordings of seizures can be made with the use of subdural grids or strips to provide additional information important in determining the optimal approach for surgical treatment (1–5).

Radiologic evaluation of metal implants is limited by streak artifacts on CT scans and by magnetic susceptibility artifacts on MR images. Despite these limitations, both techniques are useful in the detection of complications associated with the surgical procedure and the placement of subdural EEG grids. Familiarity with the normal imaging appearance of the subdural grids as well as an understanding of the associated artifacts and complications are essential in identifying and mitigating potential morbidity.

This study was performed to determine and compare the CT and MR imaging appearance of implanted subdural EEG grids and to identify the types and frequency of associated complications.

Methods

We retrospectively reviewed the medical records and imaging studies of 51 consecutive patients who underwent 54 craniotomies for grid placement at our institution between June 1988 and September 1993. (Three patients underwent two separate craniotomies each for repeat placement of grids.) Grid composition was noted for each patient; all grids used had between 20 and 128 contacts (Fig 1). The subdural grid arrays included models 2111–20–60, 2111–32–60, 2111–64–60, 2111–20P-60, 2111–32P-60, and 2111–64P-60, manufactured by the PMT Corp, Chanhassen, Minn. Both CT and MR imaging were obtained in 22 patients, 27 patients had CT only, and five

Received September 17, 1997; accepted after revision December 10.

From the Departments of Radiology (M.A.S., M.I.R., G.H.Z., M.T.Z.) and Neurology (G.K.B.), University of Maryland Medical Systems, Baltimore.

Address reprint requests to Michael Rothman, MD, Department of Radiology, University of Maryland Medical Systems, 22 S Greene St, Baltimore, MD 21201.

patients had MR imaging only. Twenty-nine patients were male and 22 were female; ages ranged from 2 to 62 years (mean age, 29 years). Thirty-two patients had primary generalized seizures and 19 had seizures resulting from an underlying structural lesion. Structural lesions included astrocytoma (n = 9), oligodendroglioma (n = 3), primitive neuroepithelial tumor (n = 2), hemangioblastoma (n = 1), arteriovenous malformation (n = 1), heterotopic gray matter (n = 1), remote infarct (n = 1), and metastatic adenocarcinoma of unknown primary origin (n = 1).

During the initial portion of the study period (21 patients with 22 procedures), the grids and connecting wires were composed of stainless steel, with a characteristic CT appearance (Fig 2). During the final portion of the study period (30 patients with 32 procedures), the grids and wires were composed of an alloy of 80% platinum and 20% iridium, with their own characteristic CT appearance (Fig 3).

Standard CT parameters for our institution were used: 1 second, 300 mA and 120 kV(p); 2 seconds, 170 mA and 120 kV(p); and 2.7 seconds, 200 mA and 133 kV(p), respectively. In all patients, contiguous axial images were obtained from the cranial base to the vertex with a section thickness of 10 mm at 10-mm intervals. Intravenous administration of 100 mL of iohexol was clinically indicated in four patients.

T1-weighted spin-echo MR sequences were obtained with parameters of 450/17/1 (TR/TE/excitations) and a section thickness of 5 to 6 mm with an intersection gap of 1 mm, or a thickness of 6 mm and a gap of 2 mm. T2-weighted images were obtained with parameters of 3500/17,90/1 or 2500/25/90/1, with a section thickness of 6 mm and an intersection gap the same as for the T1-weighted images. Intravenous administration of 0.2 mL/kg (0.1 mmol/kg) gadopentetate dimeglumine was used when clinically indicated in four patients, and the T1-weighted imaging parameters were repeated. All images were acquired with a 256 × 192 (frequency × phase encoding) matrix and a 24-cm field of view.

All studies were reviewed retrospectively for image quality and degradation by the implanted EEG grids, for intra- and extraaxial collections, and for mass effect; differences of opinion were resolved by consensus.

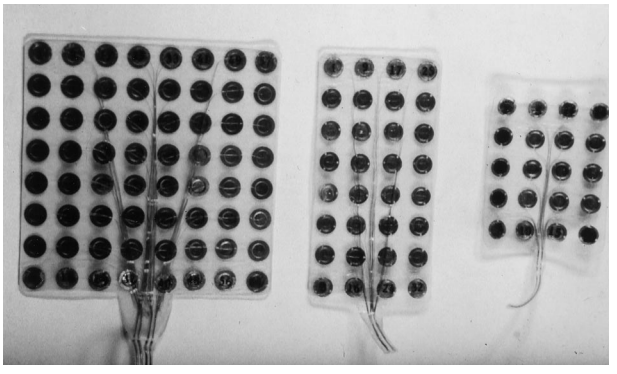

FIG 1. Subdural EEG grids ex vivo. From *left* to *right*, disk electrodes are in arrays of 8 × 8, 4 × 8, and 4 × 5 (with the connecting wires cut).

Results

Typical Imaging Appearance

The typical CT appearance of the subdural grid is a direct result of its metallic composition. The differences in appearance were due to the increased streak artifacts caused by the threefold increased density of the alloy over the stainless steel (7). The typical MR imaging appearance of the subdural grid is also a result of its metallic composition (Fig 4).

Postoperative Complications

Sixteen different complications were detected by imaging in 14 patients. Four patients had extraaxial hematomas (all patients with nonlesional seizures) (Fig 5); four patients had subfalcine or transtentorial herniations (one patient each with nonlesional seizures, astrocytoma, oligodendroglioma, and arteriovenous malformation); two patients had tension pneumocephali (both with astrocytoma) (Fig 6); two patients had extraaxial CSF collections (both without lesions); two patients had intraparenchymal hemorrhages (one with astrocytoma and one with primary seizures) (Fig 7); and one patient each had cerebritis (a patient with primary seizures) and probable brain abscess (a patient with astrocytoma) (Fig 8).

Only two patients had clinically apparent sequelae (one with tension pneumocephalus and one with transtentorial herniation). The tension pneumocephalus was tapped; the clinically evident (pupillary changes) transtentorial herniation, which occurred in an

FIG 2. CT scan after placement of stainless steel EEG grid array shows only localized streak artifact from the grid. The grid is displaced inward from the inner table of the calvaria by an epidural collection.

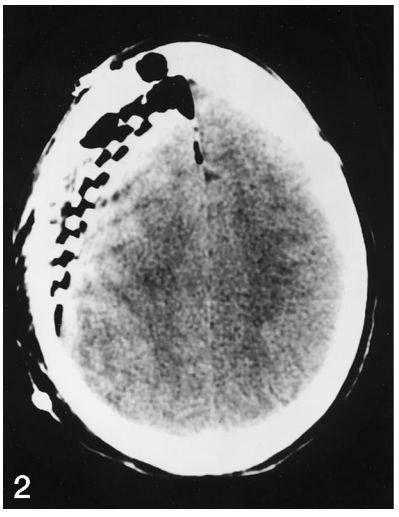

FIG 3. CT scan after placement of platinum-iridium alloy EEG grid array shows moderate streak artifact from the grid, permitting limited evaluation of intracranial structures.

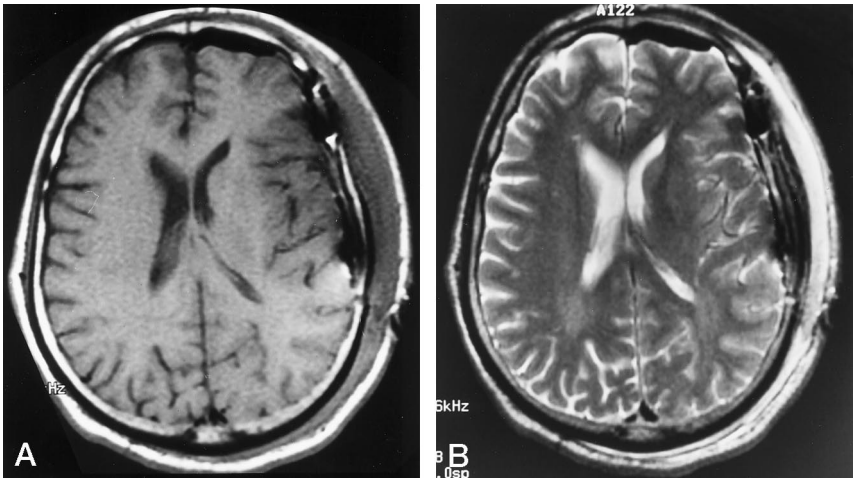

FIG 4. T1-weighted (450/17/1) (*A*) and T2-weighted (3500/17,90/1) (*B*) axial MR images of the brain after subdural EEG grid placement with platinum-iridium alloy grids on the left side.

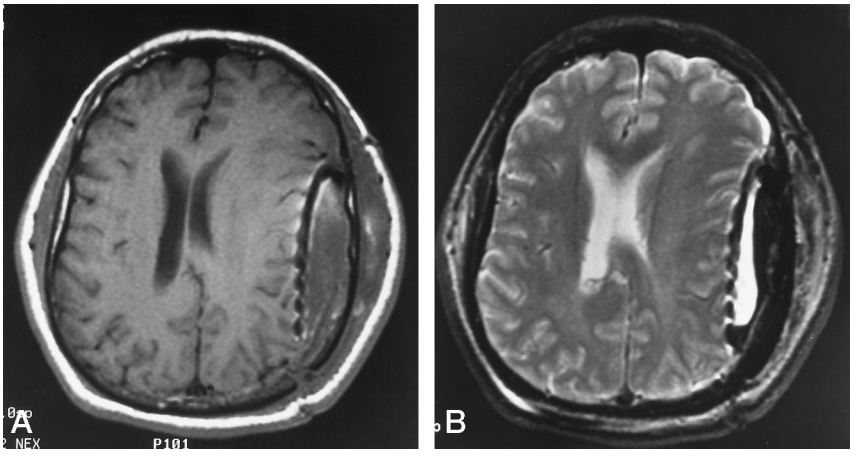

FIG 5. T1-weighted (450/17/1) (*A*) and T2-weighted (3500/17,90/1) (*B*) axial MR images of the brain after subdural EEG grid placement show a large extraaxial hematoma displacing the alloy grid array medially, with resultant midline shift.

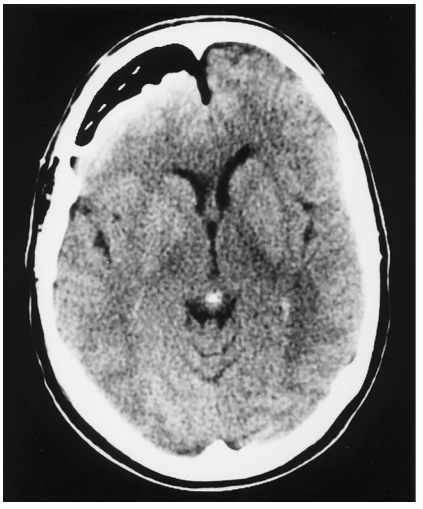

FIG 6. Axial CT scan of the brain in a patient with stainless steel grid shows right frontal extraaxial air collection exerting a mass effect on the frontal lobe, consistent with tension pneumocephalus.

FIG 7. Axial CT scan of the brain shows high-density material, consistent with acute hemorrhage, medial to the stainless steel grid in the left frontal and temporal lobes after subdural EEG grid placement, causing the brain stem to shift to the right. Hemorrhage was not apparent on preoperative studies.

FIG 8. T1-weighted (450/17/1) contrast-enhanced coronal MR image of the brain shows a right frontal ring-enhancing mass, consistent with an abscess cavity immediately deep to the site of EEG grid placement. This lesion was not present on the preoperative imaging study.

awake, alert patient with hyponatremia due to salt wasting, was successfully treated with fluid restriction. The other three patients who had transtentorial or falcine herniations detected by imaging had no clinical signs and required no specific treatment. The patient with MR imaging evidence of cerebritis had an infected subdural collection detected at the time of grid removal; however, he had no symptoms referable to this, and he was treated with an additional course of antibiotics. The patient with MR imaging evidence of an abscess received antibiotics and follow-up MR imaging, but was then lost to the service after 1 month and his long-term outcome is unknown. Two patients had radiologic evidence of substantial subgaleal fluid collections after grid placement, consistent with CSF leaks; all resolved after routine removal of the grid. Therefore, only four of the patients had complications of subdural grid placement that required specific or additional treatment other than routine antibiotics and corticosteroids. No patient required removal of the subdural grid prematurely (ie, before it could record sufficient seizures) as a result of the complications detected by imaging. One patient did have the grid removed early because of an aphasia that developed after placement. No abnormalities were noted on this patient's imaging studies, and the aphasia resolved promptly after the grid was removed. No patient had residual sequelae as a result of subdural grid placement.

Discussion

Subdural grids can detect electrical signals without the soft-tissue attenuation of electrical signals present during scalp recordings (4, 5). Unlike with the placement of subdural strips, which may be accomplished via a burr hole, placement of grids requires a craniotomy, although the brain parenchyma is not penetrated during grid placement on pial surfaces. Grids provide a larger solid angle of recording than do depth electrodes, and they cover a greater area (6). Localization of epileptic regions as well as mapping of functional cortex (eg, motor and speech areas) are facilitated by these arrays (4, 5).

After open craniotomy, one or more EEG grids are placed directly on the pial surface of the brain. The grids are composed of individual metallic disk electrodes embedded in a flat layer of Silastic. The disks are 3 to 5 mm in diameter and are separated by 10-mm center-to-center distances. There are various array sizes, including patterns of 4×4, 4×5, 4×6, 4×8, and 8×8 disks. Combinations may be used in a single patient. The electrodes are connected via electrically isolated wires that extend to insulated cables that attach to an extracranial amplifier. EEG recordings are then obtained (4, 5). Perioperatively, patients are routinely treated with antibiotics and corticosteroids.

Postoperative plain films of the skull are used to document the position of the grid and to supplement drawings or photographs made intraoperatively. Further imaging with MR or CT may be necessary after grid implantation to confirm accurate placement of the grids over the region of clinical concern or EEG abnormality, and to detect complications before surgical resection of a seizure focus.

Although patients with both stainless steel and platinum-iridium alloy grids had CT examinations, only patients with alloy grids had MR imaging. We had demonstrated that the stainless steel grids, ex vivo, torqued in the presence of a 1.5-T MR unit and were therefore susceptible to displacement, with potential injury to the patient. While not ferromagnetic, the alloy grids still possess the metallic properties necessary to conduct electrical currents for localization. Because of the grid's metallic properties, the oscillating magnetic field in the imager can induce electrical currents. By design, each disk electrode and its connecting wire are electrically isolated from the rest so as to provide precise anatomic localization of seizure foci. This isolation prevents the formation of a closed loop, and therefore electrical currents cannot be produced. Additional care must be taken to avoid skin contact with the exiting wires, as such contact could potentially close the loop, resulting in serious burns to the patient. None of the patients in our study suffered any adverse effects attributable to MR imaging.

Because of extensive streak artifacts, CT scans showed only gross abnormalities, such as large extraaxial hematomas and herniations. These artifacts were less a problem in the examination of patients with the stainless steel grids. However, these grids precluded MR imaging. Because of the desire to obtain MR imaging, the nonferromagnetic alloy grids were used extensively at our institution after their development and clinical introduction. Unfortunately, because of the threefold increase in density over the stainless steel grids, the CT artifacts were exaggerated on scans of patients with the MR imaging–compatible alloy grids. These artifacts occur because the major component of the stainless steel grids is iron, with a density of 7.87 g/cm^3, and the alloy grids are composed of platinum and iridium, with densities of 21.5 g/cm^3 and 22.6 g/cm^3, respectively (7). The artifacts seen on MR images of patients with the alloy grids were much more localized, even when compared with the CT scans of the patients with stainless steel grids, and thus provided superior representation of grid placement and associated complications.

Conclusion

The characteristic streak artifacts on CT scans are exaggerated on the studies of patients with platinum-iridium alloy grids as compared with those who have the stainless steel grids. In this study, only patients with alloy grids had MR imaging, because of observed ex vivo torquing of the stainless steel grids in a magnetic field. MR imaging artifacts were relatively more localized, aiding the evaluation and recognition of some postoperative complications that might have

remained undetected if only CT had been performed. Most of these complications detected by imaging were not apparent clinically. All complications resolved either after grid removal or with treatment; no sequelae resulted (although one patient was lost to long-term follow-up). Subdural grid recording arrays are important tools for recording seizures and for functional mapping, and they are generally well tolerated. Neuroimaging, particularly MR imaging, appears to be a sensitive means for detecting associated complications of subdural grid placement.

Acknowledgments

We thank David Crandall for preparation of the illustrations; Edie Brooks, RN, for her assistance in developing the study group; Moriel NessAiver for his excellent understanding of imaging physics; and Erma Owens, ATMA, Master Technologist, Allan Krumholz, MD, Elizabeth Barry, MD, and Aizik Wolf, MD, for their involvement in the care of the patients in this review.

References

1. Awad IA, Rosenfeld J, Ahl J, Hahn JF, Luders H. **Intractable epilepsy and structural lesions of the brain: mapping, resection strategies, and seizure outcome.** *Epilepsia* 1991;32:179–186
2. Salanova V, Morris HH, Van Ness PC, Luders H, Dinner D, Wylie E. **Comparison of scalp electroencephalogram with subdural electrocorticogram recordings and functional mapping in frontal lobe epilepsy.** *Arch Neurol* 1993;50:294–299
3. Jayakar P, Duchowny M, Resnick TJ, Alvarez LA. **Localization of seizure foci: pitfalls and caveats.** *J Clin Neurophysiol* 1991;8:414–431
4. Arroyo S, Lesser RP, Gordon B, Fischer RS, Uematsu S. **Subdural electrodes. In: Neidermeyer E, Lopes da Silva F, eds.** *Electroencephalography: Basic Principles, Clinical Applications, and Related Fields.* Baltimore: Williams & Wilkins; 1993
5. Lesser RP, Luders H, Klem G, et al. **Extraoperative cortical functional localization in patients with epilepsy.** *J Clin Neurophysiol* 1987;4:27–53
6. Barry E, Wol A, Huhn S, Bergey GK, Krumholz A. **Presurgical evaluation of patients with refractory complex partial seizures using simultaneous subdural grid and depth electrodes.** *J Epilepsy* 1992;5:111–118
7. Budaveri S, ed. *The Merck Index.* 11th ed. Rahway, NJ: Merck & Co; 1997:804–805